Fusion Engineering and Design 161 (2020) 111952

Contents lists available at ScienceDirect

Fusion Engineering and Design

journal homepage: www.elsevier.com/locate/fusengdes

Material strength standard of F82H for RCC-MRx

Hideo Sakasegawa [1,*], Hiroyasu Tanigawa, Takanori Hirose, Taichiro Kato, Takashi Nozawa

National Institutes for Quantum and Radiological Science and Technology, Rokkasho, Aomori 039-3212, Japan

ARTICLE INFO

Keywords:
Reduced-activation ferritic/martensitic steel
Material strength standard
tensile
creep
fatigue
RCC-MRx
Blanket module

ABSTRACT

Non-irradiated and irradiated material properties of a reduced activation ferritic/martensitic steel, F82H, have been extensively accumulated through international collaborative researches. F82H then demonstrates material properties applicable to the structural material of breeding blanket module. At present, material strength standard needs to be developed for the design activity of blanket module. Material strength standard generally gives average, minimum, and design values of mechanical property and their equations complying with the definition in construction code. In this work, we summarized and analyzed the experimental data of tensile, creep, and fatigue properties, and developed the material strength standard for RCC-MRx. Obtained values were then compared to those of Eurofer. Though some minor differences were observed in minimum and average values of tensile and creep properties, no significant differences were observed in their design values. As for fatigue property, F82H showed conservative design curves.

1. Introduction

Japanese RAFM (Reduced-Activation Ferritic/Martensitic) steel, F82H (Fe-8Cr-2W, V, Ta), has been studied since the late 1980s. Through international collaborative researches such as IEA (International Energy Agency) round-robin test, Japan-US collaboration test using HFIR (High Flux Isotope Reactor in Oak Ridge National Laboratory), and Japan-EU BA (Broader Approach) activities, we have extensively accumulated both non-irradiated and irradiated material properties of F82H so far. It demonstrates material properties applicable to ITER TBM (Test Blanket Module) as a milestone of DEMO blanket module.

Practical application of F82H as the structural material of blanket module needs material strength standard, which gives average, minimum, and design values and equations of mechanical properties. This standard has to be developed complying to the definition in construction codes such as RCC-MRx, ASME (American Society of Mechanical Engineering) and JSME (The Japan Society of Mechanical Engineering). This is because design activities cannot be proceeded complying to such exisiting codes which enhance public safety and technological advancement.In particular, RCC-MRx is applied to the construction code of ITER TBM. Consequently, the material strength standard of F82H should be developed complying with the definition in the latest version of RCC-MRx and including the latest data, though the material design data was reported by A.-A.F. Tavassoli, et al. basing on the data obtained through IEA round-robin test results [1].

In this work, we summarized and analyzed the data of tensile, creep, and fatigue properties, and calculated average, minimum, and design values referring to RCC-MRx 2018 [2]. These values were then compared to those of European RAFM, Eurofer (X10CrWVTa9-1) [2,3,4], which was already issued in Section III Tome 6: Probationally phase rules [2].

2. Procedures

RCC-MRx 2018 gives definitions of the design values in the chapters from A3.GEN.2 to 5 of Section III Tome 1 Subsection Z: Technical appendices. The subsequent chapters in Appendix A3 describe material strength standard. By contrast, Eurofer and some data of Mod. 9Cr-1Mo steel are separately provided in Section III Tome 6: Probationary phase rules, which defines a rule for a technical field with a current status which is insufficiently defined to permit direct inclusion in the Code [2]. In this work, material strength standard of F82H was developed referring to Section III Tomes 1 and 6.

Table 1 lists chemical composition of analyzed heats of F82H with its specification. Typical heat treatment conditions are normalizing (1040 °C for 40 min / air cooling) and temperting (750 °C for 60 min / air cooling). More detailed information for these heats are given in other

* Corresponding author.
E-mail address: sakasegawa.hideo@jaea.go.jp (H. Sakasegawa).
[1] Current affiliation: Japan Atomic Energy Agency, Kagamino, Okayama 708-0698, Japan.

https://doi.org/10.1016/j.fusengdes.2020.111952
Received 20 September 2019; Received in revised form 7 August 2020; Accepted 9 August 2020
Available online 20 August 2020

Table 1
Chemical composition of analyzed heats of F82H (wt%).

Element	Heat						
	Specification	Pre. IEA	IEA	BA07	BA10	BA11 STG	BA12
C	0.08-0.12	0.097	0.09	0.088-0.091	0.094	0.10-0.104	0.099
Si	<0.2	0.09	0.07-0.11	0.16-0.17	0.11	0.11-0.15	0.10
Mn	0.05-0.5	0.07	0.10-0.16	0.45-0.46	0.48	0.46-0.47	0.45
P	<0.02	0.002	0.002-0.003	0.009	0.005	0.0040-0.0059	0.011
S	<0.01	0.003	0.001-0.002	0.002-0.003	0.0003	0.0008-0.001	<0.0005
Cr	7.5-8.5	7.46	7.64-7.87	7.97-8.02	7.83	7.91-7.99	7.88
W	1.6-2.2	2.10	1.94-1.98	1.88	1.89	1.81-1.91	1.78
V	0.15-0.25	0.18	0.16-0.19	0.19	0.20	0.20	0.19
Ta	0.02-0.10	0.030	0.02-0.04	0.03-0.04	0.027	0.037-0.05	0.093
B	<0.006	0.0004	0.0002	0.002	0.0001	0.0003	0.0040
Ti	<0.01	0.008	0.004-0.01	<0.003	<0.002	<0.0001-<0.002	<0.001
O	<0.005	0.0033	-	0.001-0.002	0.0010	0.0020-0.0028	0.0012
N	<0.025	0.004	0.006-0.008	0.016	0.0038	0.01-0.0128	0.0098
Sol. Al	<0.04	-	0.001-0.003	0.007	0.010	0.014-0.031	0.022
Fe	Bal.	Bal.	Bal.	Bal.	Bal.	Bal.	Bal.

-: Not analyzed, Sol.: Solution, Bal: Balance.

Table 2
Number of analyzed data (7.5 ≤ t: thickness ≤ 55 mm).

Mechanical property	Heat						Total
	Pre. IEA	IEA	BA07	BA10	BA11 STG	BA12	
Tensile	0	90 [6,7,8, 13–16]	91 [14, 15, 16]	4 [12, 15, 16]	4 [15, 16]	92 [14, 15, 16]	281
Creep	81 [10, 16]	110 [6,7,8, 10,13, 16]	31 [16]	0	0	0	222
Fatigue	0	0	32 [16, 17, 18]	0	0	0	32

reports [5–18] and physical properties were already reported in [19]. In this work, Tensile, creep, and fatigue test reulsts using standard size specimens for these six different heats were summarized and analyzed to calculate material strength standard, as listed in Table 2. These data were obtained from plates with thicknesses ranging from 7.5 to 55 mm. Most of creep data was obtained using pre-IEA and IEA heats, because they have been evaluated since the beginning of IEA round-robin test [9, 11]. One of the creep rupture tests for IEA heat is still ongoing and its rupture time is more than two hundred thousand hours. By contrast, fatigue test results using standard size specimens were limited [5], because most fatigue tests have been performed using small size specimens for considering the comparison with test results after irradiation. The data of BA10 and BA11 STG heats, which meet the specification, were additionally analyzed to improve the statistical reliability of material strength standard, though their numbers of data were limited.

3. Results and discussion

3.1. Tensile property

3.1.1. Average and minimum yield strengths at 0.2% offset: $(R_{p0.2})_{ave}$ and $(R_{p0.2})_{min}$

A third degree polynomial equation of temperature (θ: temperature in Celsius degree) was fitted to all data disregarding specimen orientation to obtain the average yield strength, $(R_{p0.2})_{ave}$. The minimum yield strength curve, $(R_{p0.2})_{min}$, was then obtained by subtracting -1.96 times the standard deviation at RT (Room Temperature) of 43.3 MPa from the average yield strength curve, which derives from the 95% confidence interval. Equations describing both average and minimum curves are given below at temperatures from RT to 600 °C.

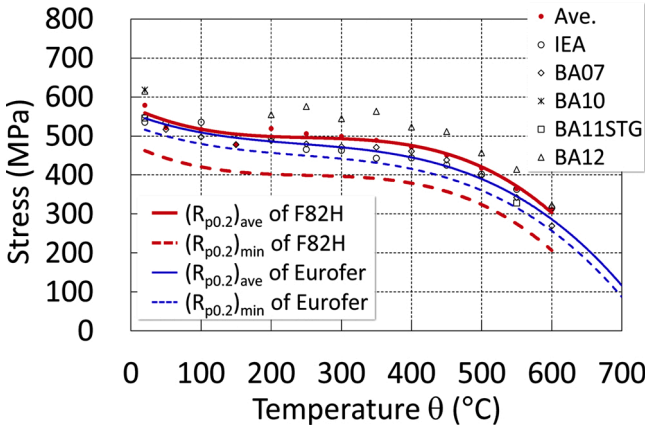

Fig. 1. Yield strength, $R_{p0.2}$.

$$(R_{p0.2})_{ave} = 574.88 - 0.85128\,\theta + 3.1951 \times 10^{-3}\,\theta^2 - 4.2186 \times 10^{-6}\,\theta^3 \quad (1)$$

$$(R_{p0.2})_{min} = (R_{p0.2})_{ave} - 1.96 \times 43.3 \quad (2)$$

These curves are shown in Fig. 1 with those of Eurofer. Average values of each heat are also given. Though the average value of F82H is higher than that of Eurofer, the minimum value is due to the larger standard deviation at RT. This mainly derives from the larger allowable range in tantalum and possible temperature fluctuations during heat treating processes.

Tantalum precipiates refine microstructures and impove mechanical properties under optimized heat treating conditions [13,20,21]. However, the precipitation behavior is susceptible to temperature fuluctuations at lower tantalum contents, which often varies mechanical properties. This is unfavorable to mass production in future [14].

Therefore, we plan to prepare next F82H heats aiming 0.1 wt% tantalum to have a stable production with a less variation of mechanical properties in addition to improved irradiation resistances [13,14]. When the allowable range of tantalum and heat treating proceses are optimized in future work focusing next heats with a higher tantalum content, the standard deviation can be lessened.

3.1.2. Average and minimum tensile strengths: $(R_m)_{ave}$ and $(R_m)_{min}$

Through the procedure similar to the yield strength values, the average tensile strength, $(R_m)_{ave}$, and minimum yield strength,

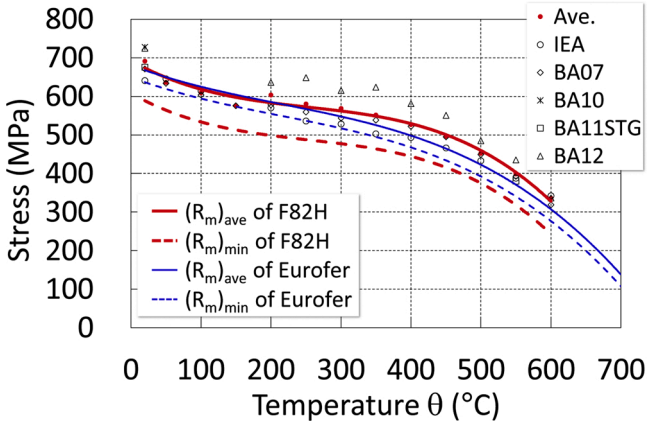

Fig. 2. Tensile strength, R_m.

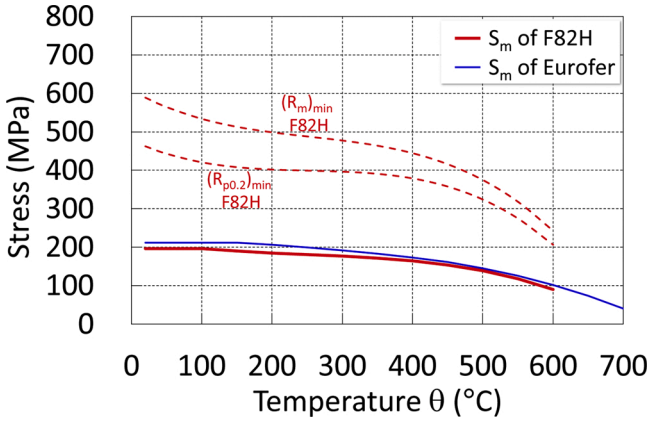

Fig. 3. S_m, Time independent maximum allowable stress.

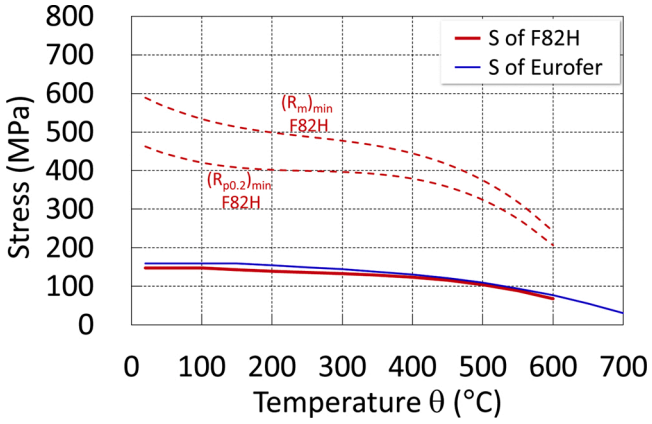

Fig. 4. S, Time independent maximum allowable stress.

$(R_{p0.2})_{min}$, were obtained. The standard deviation at RT was 49.3 MPa.

$$(R_m)_{ave} = 692.57 - 1.0191\,\theta + 3.2102 \times 10^{-3}\,\theta^2 - 4.2077 \times 10^{-6}\,\theta^3 \quad (3)$$

$$(R_m)_{min} = (R_m)_{ave} - 1.96 \times 49.3 \quad (4)$$

These curves are shown in Fig. 2 with those of Eurofer. Average values of each heat are also given. The average value of F82H is comparable to that of Eurofer, but the minimum value is lower. This derives from the same reason as yield strength.

Table 3
Time independent maximum allowable stress: S_m and S (MPa).

θ (°C)	$(R_{p0.2})_{min}$	$(R_m)_{min}$	S_m	S
20	462	589	196	147
50	443	564	196	147
100	421	534	196	147
150	408	513	190	142
200	402	499	185	139
250	399	488	181	136
300	397	477	177	133
350	391	464	172	129
400	379	444	165	123
450	358	416	154	115
500	324	375	139	104
550	275	318	118	88
600	206	243	90	68

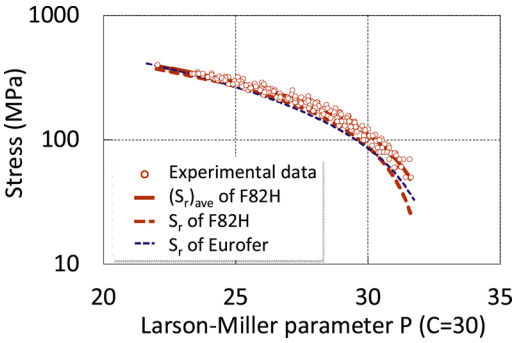

Fig. 5. Creep rupture stress, $(S_r)_{ave}$ and S_r.

3.1.3. *Time independent maximum allowable stresses: S_m and S*

Figs. 3 and 4 give time independent maximum allowable stresses, S_m and S, respectively. Their values are also given in Table 3.

Though there are differences in $(R_{p0.2})_{min}$ and $(R_m)_{min}$ between F82H and Eurofer, F82H shows less differences in S_m and S, which are comparable to or slightly lower than those of Eurofer.

3.2. *Creep property*

3.2.1. *Average and minimum creep rupture stresses: $(S_r)_{ave}$ and S_r*

A third degree polynomial equation was fitted to all data summarized using Larson-Miller parameter, P (t_r: time to rupture in hours), to obtain the average creep rupture stress, $(S_r)_{ave}$.

$$P = (\theta + 273.15) \times (\log_{10} t_r + 30) / 1000 \quad (5)$$

The minimum creep rupture stress, S_r, was then obtained by subtracting -1.96 times the standard deviation considering each condition of creep test of 11.42 MPa from the average creep rupture stress curve, $(S_r)_{ave}$ [1].

$$(S_r)_{ave} = 1043.9 - 28.989\,P + 8.8634 \times 10^{-2}\,P^2 - 5.3231 \times 10^{-3}\,P^3 \quad (6)$$

$$S_r = 1043.9 - 28.989\,P + 8.8634 \times 10^{-2}\,P^2 - 5.3231 \times 10^{-3}\,P^3 - 1.96 \times 11.58 \quad (7)$$

These curves are shown in Fig. 5 with S_r of Eurofer summarized also using Larson-Miller parameter [2]. Sr of F82H is equal to or higher than that of Eurofer except the higher Larson-Miller parameter region. It means that data of longer rupture times at lower applied stresses have to be accumulated and analyzed continuing tests.

3.2.2. *Time dependent maximum allowable stress: S_t*

From the minimum creep rupture stress, S_r, and additional analyses on creep curves, time dependent maximum allowable stress, S_t, was

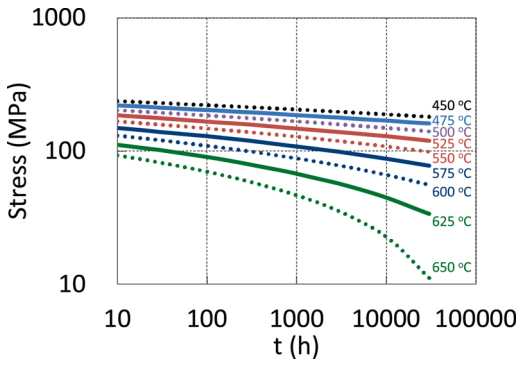

Fig. 6. S_t, Time dependent allowable stress.

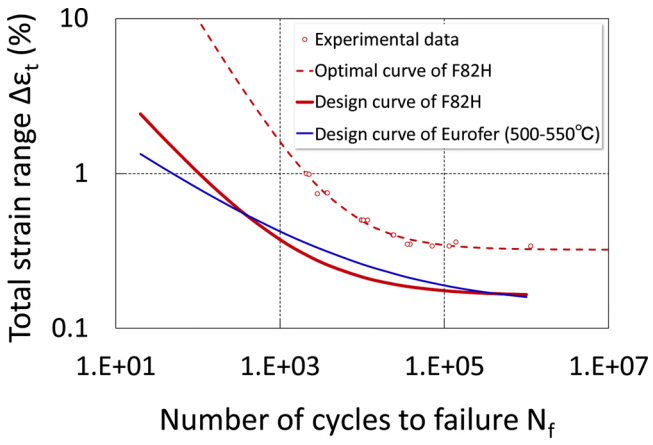

Fig. 8. Fatigue curve 550 °C.

Table 4
Time dependent maximum allowable stress, S_t (MPa).

θ (°C)	t (h)							
	10	30	100	300	1000	3000	10^4	3×10^4
450	237	230	221	214	205	197	189	181
475	220	212	203	195	186	178	169	161
500	203	194	185	177	167	159	149	140
525	185	176	167	158	148	139	129	120
550	167	158	148	139	128	119	108	99
575	149	139	129	119	108	98	88	77
600	131	121	110	99	88	78	66	56
625	112	101	90	79	68	57	45	34
650	93	82	70	59	47	35	23	11

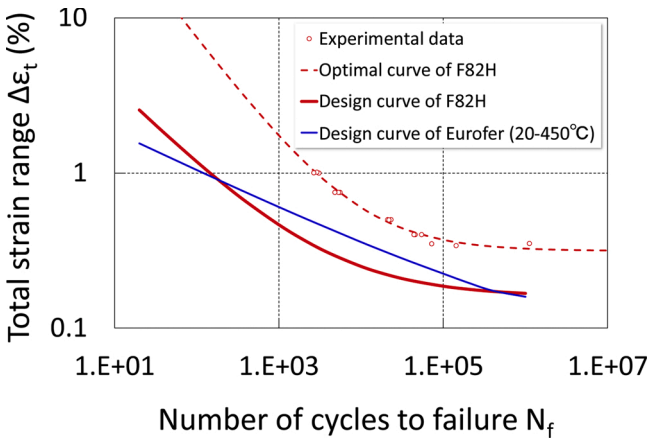

Fig. 7. Fatigue curve 400 °C.

obtained, as shown in Fig. 6. The values are also given in Table 4. The present work indicates that S_t is found to be governed by 2/3 of minimum creep rupture stress, S_r, similar to Eurofer. As aforementioned, more creep tests at longer rupture times followed by analyses have to be performed for the update of material strength standard.

3.3. Fatigue property

Langer type equation was fitted to the data of 400 and 550 °C tests to obtain their optimal fatigue curves [1]. In this work, design curve was obtained also fitting a smooth curve of Langer type equation to the minimum of curves calculated from $\Delta\varepsilon_t/2$ and $N_f/20$ of optimal curve [2], excluding the data lower than 1×10^2 and the data ranging from

Table 5
Coefficient in Langer type equation.

Temperature (°C)	Curve	$\Delta\varepsilon_t = A\,N_f^B + \Delta\varepsilon_0$		
		A	B	$\Delta\varepsilon_0$
400	Optimal	1.80	−0.700	3.13×10^{-3}
	Design	0.116	−0.527	1.59×10^{-3}
550	Optimal	5.31	−0.873	3.22×10^{-3}
	Design	0.138	−0.605	1.62×10^{-3}

Table 6
Total strain range of design curve (%).

Number of cycles	400 °C	550 °C
20	2.546	2.418
40	1.816	1.645
100	1.182	1.014
200	0.869	0.722
400	0.652	0.530
10^3	0.463	0.373
2×10^3	0.370	0.301
4×10^3	0.306	0.253
10^4	0.250	0.214
2×10^4	0.222	0.196
4×10^4	0.203	0.184
10^5	0.186	0.175
2×10^5	0.178	0.170
4×10^5	0.172	0.167
10^6	0.167	0.165

1×10^3 to 1×10^4 in number of cycles to failure in order to conservatively obtain a continuous curve. It should be noted that ASME and JSME indicate different methods to obtain fatigue curves [22].

The curves of 400 and 550 °C are shown in Figs. 7 and 8, respectively, with those of Eurofer and their coefficients of Langer type equation are given in Table 5. Table 6 lists value of design fatigue curve. As for the comparison of design curve, Eurofer shows higher total strain range except for the ranges of N_f lower than about 1×10^2 and higher than about 1×10^6.

Similarly to the case of creep properties, more fatigue tests and analyses have to be continued for the update of material strength standard. For example, a design curve can be obtained for temperatures ranging from room temperature to 400 °C similar to Eurofer [2], when no significant differences are observed between test results. Other design values of fatigue property defined in RCC-MRx, such as K_ε, K_ν, and K_s, are presented in a companion paper by T. Hirose, et al. [18].

Table 7
Gap analysis with Eurofer in RCC-MRx 2018.

Section III Tome 6: Probationally phase rules (RPP4-2012-Eurofer)		Eurofer	F82H
A.3.19AS.4	Properties for analysis – Basic		
A3.19AS.41	Conventional yield strength at 0.2% offset $R_{p0.2}$	Specified	Fig. 1
A3.19AS.42	Tensile strength R_m	Specified	Fig. 2
A3.19AS.43	Values of S_m and S	Specified	Figs. 3 and 4, Table 3
A3.19AS.44	Number not used		
A3.19AS.45	Tensile stress-strain curves		
A3.19AS.451	For plastic strain limited to 2%	Specified	Ongoing
A3.19AS.452	For total strain reaching elongation at maximum load	Specified	Ongoing
A3.19AS.46	Cyclic curves, values of K_e, K_ν, and K_s		
A3.19AS.461	Cyclic curves	Specified	Specified [18]
A3.19AS.462	Coefficient K_e	Specified	Specified [18]
A3.19AS.463	Coefficient K_ν	Specified	Specified [18]
A3.19AS.464	Symmetrisation coefficient K_s	Specified	Specified [18]
A3.19AS.47	Fatigue curves	Specified	Figs. 7 and 8, Tables 5 and 6
A3.19AS.5	Properties for analysis – creep – thermal ageing		
A3.19AS.51	Thermal ageing coefficient	Specified	Ongoing
A3.19AS.52	Values of S_t	Specified	Fig. 6, Table 4
A3.19AS.53	Creep rupture stress S_r	Specified	Fig. 5
A3.19AS.54	Creep strain rules		
A3.19AS.541	Primary creep	Specified	Ongoing
A3.19AS.542	Secondary creep	Specified	Ongoing
A3.19AS.543	End of secondary creep	Specified	Ongoing
A3.19AS.55	Fatigue-Creep interaction diagram	Specified	Ongoing
A3.19AS.56	Maximum allowable strain D_{max}	Ongoing	Ongoing
A3.19AS.6	Properties for analysis – Irradiation		
A3.19AS.61	Conventional yield strength at 0.2% offset $R_{p0.2}$ (after irradiation)	Specified	Ongoing
A3.19AS.62	Tensile strength R_m (after irradiation)	Specified	Ongoing
A3.19AS.63	Values of S_m and S (after irradiation)	Specified	Ongoing
A3.19AS.64	Ductility characteristics (before and after irradiation)	Specified	Ongoing
A3.19AS.7	Number not used		
A3.19AS.8	Properties for analysis – fracture mechanics		
A3.19AS.81	Fracture mechanics - basic		
A3.19AS.811	Values of J_{IC} and K_{IC}	Specified	Ongoing

4. Conclusions

We summarized and analyzed the data of tensile, creep, and fatigue properties, and then calculated average, minimum, and design values to develop the material strength standard of F82H for RCC-MRx. This standard is applicable to the design of blanket module made of F82H conforming to RCC-MRx after qualification processes. However there still remain some values to be specified, as listed in Table 7 of gap analysis. F82H has plenty of data accumulated through international corroborative researches and most remained values can be obtained through analyses. It is necessary to keep the material strength standard updated performing further tests and analyses. The material strength standards for other codes such as ASME and JSME should be separately developed, because some differences in definitions can be seen between codes. However, this material strength standard is helpful to develop them.

CRediT authorship contribution statement

Hideo Sakasegawa: Conceptualization, Investigation, Data curation, Formal analysis, Writing - original draft. **Hiroyasu Tanigawa:** Investigation, Supervision, Project administration. **Takanori Hirose:** Investigation, Data curation, Formal analysis. **Taichiro Kato:** Investigation, Resources. **Takashi Nozawa:** Data curation, Supervision, Writing - review & editing.

Declaration of Competing Interest

The authors report no declarations of interest.

Acknowledgments

The authors would like to express our special thanks to Dr. F. Tavassoli who gave us fruitful discussions and advice to update and develop the material strength standard F82H for RCC-MRx.

References

[1] A.-A.F. Tavassoli, J.-W. Rensman, M. Schirra, K. Shiba, Materials design data for reduced activation martensitic steel type F82H, Fusion Eng. Des. 61-62 (2002) 617–628.
[2] AFCEN, RCC-MRx 2018.
[3] F. Tavassoli, Eurofer Steel, Development to Full Code Qualification, Procedia Eng. 55 (2013) 300–308.
[4] E. Gaganidze, F. Gillemot, I. Szenthe, M. Gorley, M. Rieth, E. Diegel, Development of EUROFER97 database and material property handbook, Fusion Eng. Des. 135 (2018) 9–14.
[5] H. Tanigawa, E. Gaganidze, T. Hirose, M. Ando, S.J. Zinkle, R. Lindau, E. Diegele, Development of benchmark reduced activation ferritic/martensitic steels for fusion energy applications, Nucl. Fusion 57 (2017), 092004.
[6] A.-A.F. Tavassoli, E. Diegele, R. Lindau, N. Luzginova, H. Tanigawa, Current status and recent research achievements in ferritic/martensitic steels, J. Nucl. Mater. 455 (2014) 269–276.
[7] H. Tanigawa, K. Shiba, A. Möslang, R.E. Stoller, R. Lindau, M.A. Sokolov, G. R. Odette, R.J. Kurtz, S. Jitsukawa, Status and key issues of reduced activation ferritic/martensitic steels as the structural material for a DEMO blanket, J. Nucl. Mater. 417 (2011) 9–15.
[8] S. Jitsukawa, M. Tamura, B. van der Schaaf, R.L. Klueh, A. Alamo, C. Petersen, M. Schirra, P. Spaetig, G.R. Odette, A.A. Tavassoli, K. Shiba, A. Kohyama, A. Kimura, Development of an extensive database of mechanical and physical properties for reduced-activation martensitic steel F82H, J. Nucl. Mater. 307–311 (2002) 179–186.
[9] Report of IEA Workshop on Reduced Activation Ferritic/Martensitic Steels, Tokyo, Japan, 2–3 November (2000) (JAERI-Conf 2001-2007), 2007.
[10] T. Nakata, H. Tanigawa, K. Shiba, S. Komazaki, M. Fujiwara, A. Kohyama, Evaluation of Creep Properties of Reduced Activation Ferritic Steels, J. Jpn. Inst. Met. 71 (2007) 239–243.
[11] H. Tanigawa, K. Shiba, H. Sakasegawa, T. Hirose, S. Jitsukawa, Technical issues related to the development of reduced-activation ferritic/martensitic steels as structural materials for a fusion blanket system, Fusion Eng. Des. 86 (2011) 2549–2552.
[12] H. Sakasegawa, H. Tanigawa, H. Tanigawa, T. Hirose, Effect of potential factors in manufacturing process on mechanicalproperties of F82H, Fusion Eng. Des. 89 (2014) 1684–1687.
[13] K. Shiba, H. Tanigawa, T. Hirose, T. Nakata, Development of the toughness-improved reduced-activation F82H steel for demo reactor, Fusion Sci. Technol. 62 (2012) 145–149.
[14] H. Sakasegawa, H. Tanigawa, S. Kano, H. Abe, Material properties of the F82H melted in an electric arc furnace, Fusion Eng. Des. 98-99 (2015) 2068–2071.
[15] H. Sakasegawa, H. Tanigawa, Mechanical properties of F82H plates with different thicknesses, Fusion Eng. Des. 109-111 (2016) 1724–1727.
[16] H. Sakasegawa, T. Kato, Y. Watanabe, H. Tanigawa, T. Hirose, Current status of the development of reduced activation ferritic/martensitic steel F82H material strength standard, Atomic Energy Society of Japan, 2018 Fall Meeting, Okayama, Japan, 5-7 September (2018).
[17] T. Hirose, H. Sakasegawa, M. Nakajima, T. Kato, T. Miyazawa, H. Tanigawa, Effects of test environment on high temperature fatigue properties of reduced activation ferritic/martensitic steel, F82H, Fusion Eng. Des. 136 (2018) 1073–1076.
[18] T. Hirose, T. Kato, H. Sakasegawa, H. Tanigawa, Evaluation of fatigue properties of reduced activation ferritic/martensitic steel, F82H for development of design criteria, Fusion Eng. Des. 160 (2020) in press.
[19] T. Hirose, T. Nozawa, R.E. Stoller, D. Hamaguchi, H. Sakasegawa, H. Tanigawa, H. Tanigawa, M. Enoeda, Y. Katoh, L.L. Snead, Physical properties of F82H for fusion blanket design, Fusion Eng. Des. 89 (2014) 1595–1599.
[20] Hideo Sakasegawa, Hiroyasu Tanigawa, Sho Kano, Masato Enomoto, Precipitation behavior in F82H during heat treatments of blanket fabrication, Fusion Eng. Des. 86 (2011) 2541–2544.
[21] Hideo Sakasegawa, Hiroyasu Tanigawa, Dai Hamaguchi, Application of various observational techniques to the characterization of MX in F82H, J. Nucl. Sci. Technol. 55 (2018) 1163–1171.
[22] The Japan Society of Mechanical Engineers, Codes for Nuclear Power Generation Facilities – Rules on Design and Construction for Nuclear Power Plants -, JSME S NC2 - 2012, 2012.